

VIII- II -1. Project Research

Project 10

Y. Ohkubo

Research Reactor Institute, Kyoto University

Objective and Participating Research Subjects

The main objectives of this project research are the investigation of the nuclear structure of unstable neutron-rich nuclei and also the local properties of materials using short-lived radioactive nuclei.

This period is the first year of the project. Unfortunately, the operation of the reactor was one week delayed and moreover the operation time of the KUR-ISOL was shortened because of some time taken to fix a vacuum leak during the reactor operation.

The research subjects (PRS) executed in this period are as follows:

PRS-1 Newly Available Fission Products at KUR-ISOL (II) (A. Taniguchi *et al.*).

PRS-2 Coincidence Summing Correction of Total Absorption Clover Detector for Determination of γ -Ray Intensities of Fission Products (M. Shibata *et al.*).

PRS-3 Half-Life Measurements of Excited Levels in ^{149}Nd (Y. Kojima *et al.*).

PRS-4 (a) Local Association of Aluminum Impurities Doped in Zinc Oxide; (b) Irradiation Effect on the Formation of Defects in Silicon Observed by the Positron Annihilation Spectroscopy (Y. Ohkubo *et al.*).

PRS-5 ^{197}Au Mössbauer Study of Au Nanoparticles (M. Seto *et al.*).

PRS-6 Elucidation of a Correlation between Magnetic Properties and Guest Inclusion in Magnetically Bistable Porous Coordination Polymers (M. Ohba *et al.*).

PRS-7 Characterization of Gold Nanoparticles Supported on Nickel Oxide by ^{197}Au Mössbauer Spectroscopy: Detection of Gold Alloy (T. Yokoyama *et al.*).

Main Results and Contents of This Report

In order to extend usable radioactive ion beams at KUR-ISOL, A. Taniguchi *et al.* (PRS-1) searched for heavy In isotopes and have confirmed that $^{126, 127, 128}\text{In}$ with half-lives of ~ 1 s (the heaviest stable isotope of In is ^{115}In) were extracted with intensities enough for nuclear spectroscopic experiments.

In order to obtain γ -ray intensities from fission products, which are important data for decay heat estimation, Y. Shima *et al.* (PRS-2) determined the peak efficiency in the energy range of 50-3200 keV for their total absorption clover detector composed of 4 large Ge crystals by measuring singles and multiple γ -rays emitters. The derived peak efficiency was found to agree with a simulated one using GEANT4, the coincidence summing correction having been done for the multiple γ -rays emitters.

The half-life of the nucleus is one of clues to understanding nuclear structure. Using a radiation detection system consisting of a high-purity Ge detector, one thin plastic and one LaBr_3 scintillators, Y. Kojima *et al.* (PRS-3) measured the half-lives of the 221-keV level, the 271-keV, and other three levels of ^{148}Nd , its parent ^{148}Pr being obtained at KUR-ISOL: $t_{1/2}$ (221-keV level) = 1.60(4) ns and $t_{1/2}$ (271-keV level) = 450(15) ps. The former result is due to the slope method, and the latter both the slope and centroid methods.

Zinc oxide, a semiconductor with a relatively large band gap, has several favorable properties in materials science. S. Komatsuda *et al.* (PRS-4a) took room-temperature TDPAC spectra of ^{111}Cd ($\leftarrow^{111}\text{In}$) introduced in 10 at.% and 10 ppm Al-doped ZnO, the patterns of which are identical with each other. Together with the XRD pattern of 0.5 at.% Al-doped ZnO, they concluded that even ppm-level Al impurities formed ZnAl_2O_4 .

Aiming at investigating the state of being and stability of impurities in semiconductors, W. Sato *et al.* (PRS-4b) took room-temperature positron lifetime spectra for high-purity single-crystalline silicon wafers nonirradiated and irradiated with γ -rays, and those irradiated with neutrons. They observed that a part of the positrons in the Si irradiated with neutrons had a longer lifetime than those in the others.

Y. Kobayashi *et al.* (PRS-5) measured at 13 K the ^{197}Au -Mössbauer spectra for $\text{Au}_{25}(\text{SG})_{18}$ (SG = glutathione) nanoparticles and those placed on a Au foil in order to obtain information on the nature of the Au atomic bonds in the nanoparticle and among the nanoparticles. They obtained the result implying that the Au atomic bonds were weak or the nanoparticles moved easily in the sample.

A porous coordination polymer, $\text{Fe}^{\text{II}}(\text{pz})[\text{Pd}^{\text{II}}(\text{CN})_4]$ (pz = pyrazine), exhibits a spin transition near room temperature with a hysteresis width of 20 K ($T_c^\uparrow = 304$ K and $T_c^\downarrow = 284$ K). When iodine is included in the pores of the polymer as a guest, the hysteresis width increases 117 K. M. Ohba *et al.* (PRS-6) investigated the chemical states of iodine using ^{129}I -Mössbauer spectroscopy at 15 K on the iodine clathrate (low-spin state) and its analog $\text{Ni}^{\text{II}}(\text{pz})[\text{Pd}^{\text{II}}(\text{CN})_4]$ (high-spin state). They obtained the results indicating that the iodine interacted with various sites in the pores and that its charge fluctuation originated from different host-guest interactions.

As a characterization of supported gold catalysts, H. Ohashi *et al.* (PRS-7) applied ^{197}Au -Mössbauer spectroscopy to obtain information of the chemical state of gold nanoparticles supported on nickel oxide. From the Mössbauer spectrum for Au/NiO_x (H_2), they considered that AuNi_x alloy phases were formed by hydrogen reduction.

A. Taniguchi, Y. Ohkubo, M. Tanigaki, H. Hayashi¹, M. M. Shibata² and Y. Kojima²

Research Reactor Institute, Kyoto University

¹School of Health Sciences, The University of Tokushima Graduate School

²Radioisotope Research Center, Nagoya University

INTRODUCTION: For the studies of nuclear structure and the application of radioactive-ion (RI) beams to other fields, the variety, energy, intensity, etc. of usable RI beams are important characteristics of RI beam facilities. Here at KUR-ISOL (Kyoto University Reactor-Isotope Separator On-Line), we are trying to extend usable RI beams. In the previous period, we successfully obtained beams of RI with sub-second half-lives, which are very short for ISOL coupled to a gas-jet system like KUR-ISOL [1]. In this period, ionization and extraction of indium isotopes in the neighborhood of a proton closed shell $Z = 50$ was focused. Although it is considered that indium atoms can be ionized using a surface ionization type of ion source [2], which is adopted for KUR-ISOL, it has never been attempted to extract indium isotopes at KUR-ISOL and therefore their availability was unknown.

EXPERIMENTS: Indium isotopes were obtained as fission products of 50-mg $^{235}\text{UF}_4$ irradiated at KUR-ISOL under the 1 MW reactor operation. The produced fission products were transported using the He/N₂ gas-jet system to the ion source. The ionized activities were mass-separated using an electromagnet and collected on an aluminized Mylar tape, and the yields were measured by detecting representative γ -rays with a Ge detector of about 30% relative efficiency. The Ge detector was placed at an in-beam position and the distance from the source to the detector was 3 cm. The optimal values of the magnetic field for the indium ions were not known although they could be estimated. Thus, the magnetic field was increased stepwise (0.1 G/300 s) from the initial value for $A \approx 125$ while monitoring γ -rays.

RESULTS: Fig. 1(a), (b) and (c) show the γ -ray energy spectra for the mass number $A = 126$, 127 and 128, respectively. As seen in these spectra, the representative γ -rays of ^{126}In ($T_{1/2} = 1.64$ s and 1.60 s), ^{127}In ($T_{1/2} = 3.66$ s and 1.09 s) and the daughter nuclide, and ^{128}In ($T_{1/2} = 0.72$ s and 0.84 s) were observed clearly. Thus, the ionization and extraction of $^{126, 127, 128}\text{In}$ were confirmed.

CONCLUSION: In order to extend usable RI beams at KUR-ISOL, ionization and extraction of indium isotopes

was tried by carefully tuning the magnetic field and the ion source, and $^{126, 127, 128}\text{In}$ beams were successfully obtained. The beam intensities were relatively strong and could be enough for their nuclear spectroscopy experiments. Moreover, it might be possible to obtain a beam of ^{129}In , which is closer to a doubly magic nucleus ($Z = 50$, $N = 82$) under the 5 MW reactor operation.

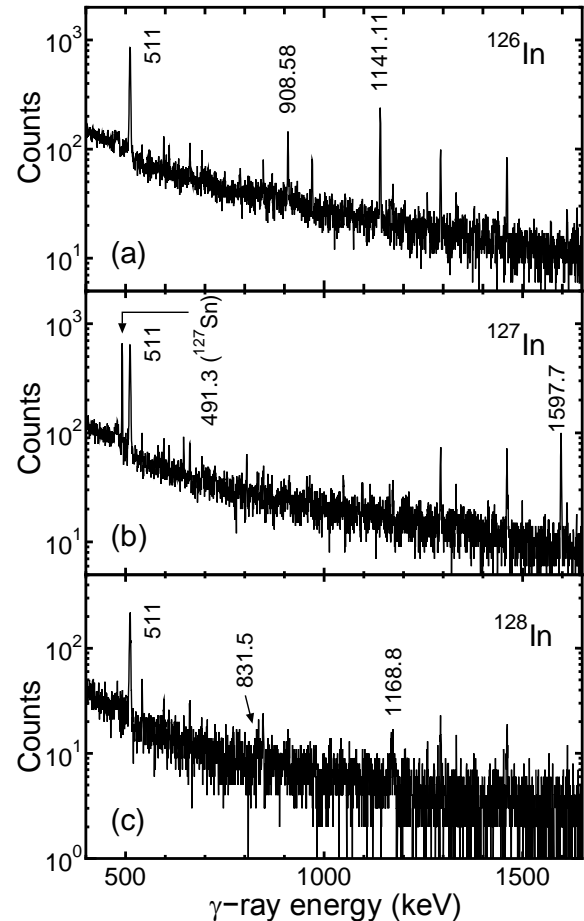


Fig. 1. The γ -ray spectra for (a) $A = 126$, (b) $A = 127$ and (c) $A = 128$. Their representative γ -rays were observed. The magnetic fields for these spectra were 3199 G, 3210 G and 3220 G, and the accumulation times were 20 min, 15 min and 5 min, respectively.

REFERENCES:

- [1] A. Taniguchi *et al.*, KURRI Prog. Rep. **2010** (2011) 90.
- [2] K. Blaum, Phys. Rep. **425** (2006) 1-78.

PR10-2 Coincidence Summing Correction of Total Absorption Clover Detector for Determination of γ -Ray Intensities of Fission Products

Y. Shima, Y. Kojima¹, H. Hayashi², A. Taniguchi³ and M. Shibata¹

Graduate School of Engineering, Nagoya University

¹Radioisotope Research Center, Nagoya University

²Institute of Health Biosciences, The University of Tokushima Graduate School

³Research Reactor Institute, Kyoto University

INTRODUCTION: Precise nuclear decay data of fission products are important for the decay heat calculations. In our previous work, γ -rays following the decay of ¹⁴⁷La were measured using a total absorption clover detector. We newly identified 56 excited levels from 1.0 to 3.5 MeV and 160 γ -rays [1], and demonstrated that the detector was useful for the identification of high energy levels and γ -rays. In this report, the peak efficiency of the detector for a wide energy region was determined in order to deduce γ -ray intensities. We measured multiple γ -ray emitters and determined the efficiencies corrected for the coincidence summing based on the decay scheme information. We verified that the coincidence summing correction was properly performed.

EXPERIMENTS AND SIMULATIONS: The detector has four large Ge crystals and a through hole along the central axis of the detector. Radioactive sources can be put into the through hole. In this measurement, two spectra, a singles and an add-back spectrum, were obtained. In the singles spectrum, four individual spectra of Ge crystals were summed and stored. In the add-back spectrum, energy signals from the different crystals corresponding to coincident events were summed and then stored. Peak efficiencies were determined using singles spectrum.

The measurements were carried out as follows. First, single γ -ray emitters of ⁵⁴Mn, ¹⁰⁹Cd, ¹³⁷Cs and ²⁰³Hg (88 - 834 keV) were measured. A peak and a total efficiency were calculated using the Monte-Carlo simulation code GEANT4. In this calculation, the diameters and lengths of Ge crystals were adjusted in order to reproduce the efficiencies obtained with the single γ -ray emitters. Next, we measured multiple γ -ray emitters of ⁵⁶Co, ¹³³Ba and ¹⁵², ¹⁵⁴Eu (53 - 3253 keV). The coincidence summing correction was applied for peak efficiencies obtained with these nuclides. In order to absorb β -rays, radioactive nuclides were sandwiched between a pair of 7-mm thick plastic β -ray absorbers.

SUMMING CORRECTION: The summing correction was performed with the Monte-Carlo calculation based on the decay schemes [2]. First, an excited level where a β -ray feeds was determined using β -branching ratios. Second, decay paths of cascade γ -rays were simu-

lated using γ -ray intensities, cascade relation of γ -rays and conversion coefficients. In the electron capture decay and the internal conversion processes, emission of fluorescence K X-rays was also taken into account, while Auger electrons and other X-rays were neglected. Third, interactions of each γ -ray or X-ray with the Ge crystals were determined with the simulated peak and total efficiency. Consequently, we obtained two calculated spectra. One is the spectrum with no coincidence summing effects. The other is the spectrum including coincidence summing effects. The correction factors were deduced by taking the ratios of peak counts between the two spectra.

RESULTS: Fig. 1 shows the peak efficiencies of the clover detector. Crosses indicate the peak efficiencies obtained with single γ -ray emitters. The simulated efficiency using the GEANT4 is shown by the solid curve. The efficiency was in good agreement with those for the single γ -ray emitters. The open and closed marks indicate the experimental and corrected peak efficiencies obtained with the multiple γ -ray emitters. The corrected efficiencies were in agreement with the simulated efficiency within 5%.

CONCLUSIONS: The coincidence summing correction was properly performed with the decay scheme information. The peak efficiency from 50 to 3200 keV was determined using single γ -ray emitters, the Monte-Carlo simulation with the GEANT4 and multiple γ -ray emitters corrected for the coincidence summing. A determination of γ -ray intensities of ¹⁴⁷La is now in progress.

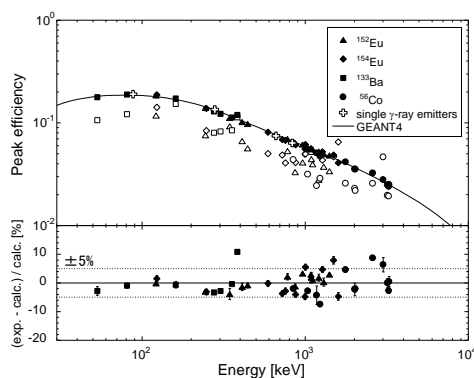


Fig.1. The full energy peak efficiency of the clover detector.

REFERENCES:

- [1] Y. Shima *et al.*, Proc. the 2011 Symposium on Nuclear Data, Tokai, Japan, Nov. 16-17, 2011, in press.
- [2] Evaluated Nuclear Structure Data File (ENSDF), <http://nndc.bnl.gov/ensdf>.

採択課題番号 23P10-2 オンライン同位体分離装置を用いた核分裂生成物の崩壊核データ測定 プロジェクト

(名大・RIC) 柴田理尋、小島康明 (名大院・工) 嶋 洋佑 (名大・工) 永井悠太、山本晃一郎
(徳島大・医) 林 裕晃 (京大・原子炉) 谷口秋洋

Y. Kojima, Y. Shima¹, H. Hayashi², A. Taniguchi³ and M. Shibata

Radioisotope Research Center, Nagoya University

¹Graduate School of Engineering, Nagoya University

²Institute of Health Biosciences, The University of Tokushima Graduate School

³Research Reactor Institute, Kyoto University

INTRODUCTION: Half-lives of excited levels are one of the most important properties in discussing nuclear structure. In the previous works, we have developed a new spectrometer consisting of a LaBr_3 and plastic scintillation detector, and successfully obtained half-lives of excited levels in ^{148}Pr in a range of nanosecond using the β - γ decayed coincidence technique [1].

In this report, we present level half-life measurements for ^{149}Nd in a range down to sub-nanosecond. The centroid shift method was also applied to deduce short half-lives.

EXPERIMENTS: The ^{149}Pr isotopes were prepared at KUR-ISOL, following the thermal neutron-induced fission of ^{235}U . The mass-separated beams were implanted into an aluminized Mylar tape, and periodically moved to a measuring port. At the detector station, the LaBr_3 , plastic scintillator and an HPGe detector were placed in a close geometry. 1.7×10^8 events were accumulated in a list mode during a measuring period of 42 h.

RESULTS AND DISCUSSION: Fig.1(a) shows the decay curve of the 221 keV level. It was obtained through gating on the 112 keV γ -ray measured with the LaBr_3 detector and on 109 keV γ -rays measured with the Ge detector. A long slope is clearly observed in the spectrum. From the least-squares fitting method using an exponential function, a half-life of 1.60(4) ns was deduced for this level. Our result agrees with the published half-life of 2.1(5) ns [2], having a much improved precision.

Fig.1(b) shows the time distribution obtained through gating on the 162 and 109 keV γ -rays. From the slope, the half-life of 453(15) ps was derived for the 271 keV level. Here, it is generally agreed that the slope method can deduce half-lives down to $\sim 1/3$ of time resolutions (FWHM) [e.g. 3]. Because the FWHM of our system is 550 ps for 165 keV, our results deduced from the slope have sufficient reliability. Moreover, it is worthwhile analyzing the data on the basis of the centroid shift method, which enables half-life determination in a range down to $\sim 1/100$ of FWHM in good statistical conditions [3].

Centroids were evaluated for time distribution curves observed in the decay of ^{149}Pr . As shown in Fig.2, most of the centroids smoothly vary with the γ -ray energy. The solid line shown in this figure is the best-fit quadratic curve. We assume that this line represents the energy dependence of centroids of prompt time distributions. In

Fig.2, the centroid deduced from the decay curve of the 271 keV level was also plotted. The difference from the prompt curve corresponds to the mean lifetime of the level. From the centroid shift, the mean life of 560(95) ps (half-life of 390(65) ps) was deduced. It is in agreement with the half-life of 453(15) ps obtained by the slope method. The weighted mean of 450(15) ps was adopted for the 271 keV level. This value is much smaller than the previous value of 5.1(3) ns [4], which was deduced from the time distribution curve of the 162 keV γ -ray. The reason for this discrepancy is uncertain, but contribution due to other levels or contamination of neighboring isotopes in the previous work is possible explanation.

New half-life values for other 3 levels in ^{149}Nd will also be deduced from the centroids, while the data are not reported here because they are tentative. Further analysis and discussion from the view point of nuclear physics are now in progress.

CONCLUSIONS: Half-lives of excited levels in ^{149}Nd were measured using the LaBr_3 detector in a range of a few hundreds picosecond.

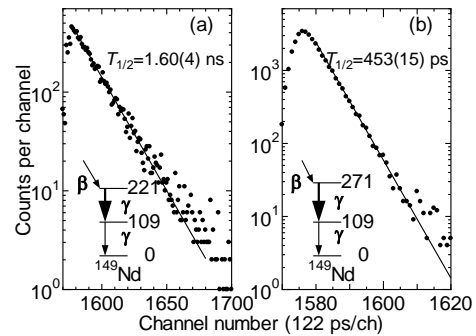


Fig.1. (a) Decay curves of the 221 keV level and (b) 271 keV level in ^{149}Nd . Gamma-rays gated by the LaBr_3 detector are shown by a thick arrows.

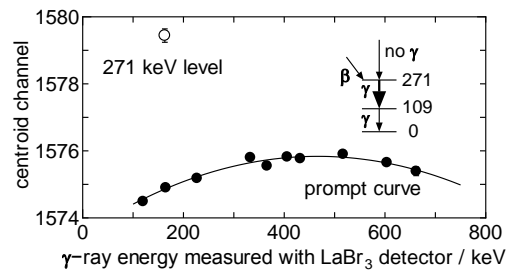


Fig.2. Centroids of time distribution curves observed in the β -decay of ^{149}Pr .

REFERENCES:

- [1] Y. Kojima *et al.*, Nucl. Instr. Meth. A **659** (2011) 193-197.
- [2] Evaluated Nuclear Structure Data File (ENSDF), <http://www.nndc.bnl.gov/ensdf>.
- [3] A. Schwarzschild, Nucl. Instr. Meth. **21** (1963) 1-16.
- [4] R. Katajanheimo *et al.*, Phys. Scr. **20** (1979) 125-128.

S. Komatsuda, W. Sato¹, S. Kawata² and Y. Ohkubo³

Graduate School of Natural Science and Technology,
Kanazawa University

¹Institute of Science and Engineering, Kanazawa University

²Department of Chemistry, Faculty of Science, Fukuoka University

³Research Reactor Institute, Kyoto University

INTRODUCTION: Zinc Oxide (ZnO) doped with group 13 elements (Al, Ga, In) as impurity donors is expected to be applied to functional devices as *n*-type semiconductors. For a practical use of ZnO as a conduction-controlling device, it is of great importance to study the physical and chemical states of dilute impurity ions in ZnO, and for that purpose, the time-differential perturbed angular correlation method (TDPAC) is very suited because it can directly provide atomic-level information of impurity atoms. In our previous work, we made a successful observation that the ¹¹¹Cd(\leftarrow ¹¹¹In) probe is locally associated with Al ion(s) even at as extremely low concentration as 0.1 ppm of Al, while the ¹¹¹Cd(\leftarrow ^{111m}Cd) probe has little interaction with Al atoms doped at a high concentration of 10 at.% [1, 2]. Our next interest is to elucidate the dispersion state of Al ions in ZnO. Taking the above contrastive observations as a clue to the local structure formed by Al impurities, in the present work, we further investigated interacting nature between the ¹¹¹Cd(\leftarrow ¹¹¹In) probe and Al impurities doped in ZnO matrix. We here discuss local environment of Al atoms based on the results of XRD and TDPAC measurements.

EXPERIMENTS: In this work, ZnO doped with two different Al concentrations (10 ppm and 10 at.%) were prepared. Stoichiometric amounts of Al(NO₃)₃·9H₂O and ZnO powder were mixed in ethanol. The suspension was heated to evaporate the ethanol until dryness. The powders were pressed into disks and sintered in air at 1273 K for 3 h. An XRD measurement was performed for one of the prepared samples doped with 10 at.% Al. For TDPAC measurements, commercially available ¹¹¹In solution was added in droplets onto each of the sintered disks with the different Al concentrations. The disks again underwent heat treatment in air at 1373 K for 2 h. The TDPAC measurements were carried out for the 171-245 keV cascade γ rays of ¹¹¹Cd(\leftarrow ¹¹¹In) probe with the intermediate state of *I* = 5/2 having a half-life of 85.0 ns.

RESULTS: Fig. 1 shows the TDPAC spectra of ¹¹¹Cd(\leftarrow ¹¹¹In) probe in (a) 10 at.% and (b) 10 ppm Al-doped ZnO. The directional anisotropy on the ordinate, $A_{22}G_{22}(t)$, was deduced with the following simple operation for delayed coincidence events of the cascade:

$$A_{22}G_{22}(t) = \frac{2[N(\pi, t) - N(\pi/2, t)]}{N(\pi, t) + 2N(\pi/2, t)} \quad (1)$$

Here, *A* denotes the angular correlation coefficient, *G*(*t*) the time-differential perturbation factor as a function of the time interval, *t*, between the relevant cascade γ -ray emissions, and *N*(θ , *t*) the number of the coincidence events observed at angle, θ . The spectral patterns and the obtained nuclear quadrupole frequencies for both samples are in good agreement with each other. These results suggest that the local structures formed by the Al ions at the probe sites are quite alike regardless of the large difference of Al concentrations. Meanwhile, as for the XRD measurement for 10 at.% Al-doped ZnO, we found that there emerged a spinel phase of ZnAl₂O₄ in ZnO. Taking into account our previous observation that the XRD pattern of 0.5 at.% Al-doped ZnO shows only peaks corresponding to a wurtzite structure of ZnO [3], the present experimental results show that even ppm-level dilute Al impurities can locally associate with each other to form such minute ZnAl₂O₄ grains that are undetectable within XRD detection precision.

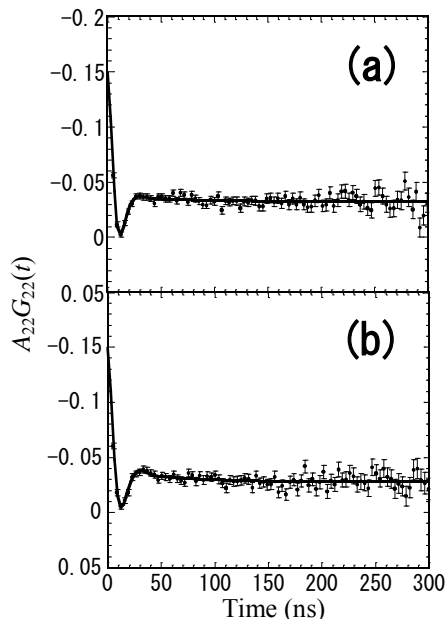


Fig. 1. TDPAC spectra of ¹¹¹Cd(\leftarrow ¹¹¹In) in (a) 10 at.% and (b) 10 ppm Al-doped ZnO.

REFERENCES:

- [1] S. Komatsuda *et al.*, KURRI Prog. Rep. **2010** (2011) 94.
- [2] S. Komatsuda *et al.*, J. Phys. Soc. Jpn. **80** (2011) 095001.
- [3] W. Sato *et al.*, Proc. Radiochim. Acta **1** (2011) 435.

W. Sato, T. Togimitsu¹, R. Ono¹ and Y. Ohkubo²*Institute of Science and Engineering, Kanazawa University*¹*Graduate School of Science and Technology, Kanazawa University*²*Research Reactor Institute, Kyoto University*

INTRODUCTION: Positron annihilation lifetime spectroscopy (PALS) is one of the most powerful tools for the study on defects formed in various solid-state materials. Among wide practical applications, this method is made use of especially for the estimation of the concentrations, sizes, and types of lattice defects in such materials as semiconductors and reactor materials. As for semiconductors, lattice defects play important roles for their electric conductivity; from this point of view, it is of great importance to investigate the state of being and stability of impurities in semiconductors by means of the present spectroscopy.

As part of our impurity-related studies using radiations as probes, we have started up research on lattice defects in matter by the positron annihilation method. In the present study, our interest was directed to lattice defects formed in single-crystalline silicon (Si) by radiation irradiation. Here, preliminary results of decay-rate change of positron annihilations caused by radiation damage are presented.

EXPERIMENTS: A ²²Na (as in NaCl) positron source of about 3 MBq covered with a Mylar film was sandwiched with high purity (99.999%) single-crystalline Si wafers with a size of 14 × 14 × 0.5 mm³. The positron annihilation lifetime was measured with a conventional circuit at room temperature, and BaF₂ scintillators were used for the detection of 1275- and 511-keV γ rays. After the measurement, the wafers were exposed to a γ -ray field at the absorbed dose rate in air of 2.76 kGy/h for 48 h at the ⁶⁰Co γ -ray irradiation facility of KURRI. Aside from the exposure to the γ -ray field, an identical type of Si wafers were irradiated for 1 h with thermal neutrons at the fluence rate of 2.75×10^{13} cm⁻² s⁻¹ at KUR. After the irradiations, PALS measurements were again carried out for the Si wafers at room temperature. For the analysis of the positron lifetime spectra, LT10 program was adopted [1].

RESULTS: In Fig. 1 is shown the PALS spectra obtained for the Si wafers (a) nonirradiated, (b) exposed to the γ -ray field, and (c) irradiated with thermal neutrons. All the spectra are made up of three different decay components as numbered 1-3. The lines 4 stand for the total of the three. Components 1 and 2 originate from

the self absorption in the source materials: the Mylar films and NaCl salt, respectively. Component 3 corresponds to positron annihilations in the Si wafers. It is obvious from the slopes of the decay curves of Component 3 that the lifetime of positrons in the Si irradiated with neutrons are longer than the others. This observational result should arise from the effect of radiation damage caused by the neutron irradiation. We thus further decomposed the component into two different ones. Including the subcomponents, lifetimes obtained for Component 3 are listed in Table 1. The longevity of the positrons in the Si irradiated with neutrons could be attributed to their trap in vacancies formed, for instance, by the recoil effect of the (*n*, γ) reactions. As for the Si exposed to the γ rays of ⁶⁰Co, however, little change was observed in the decay rate. This may be because the energies of the relevant γ rays would not be enough to cause radiation damages irrecoverable.

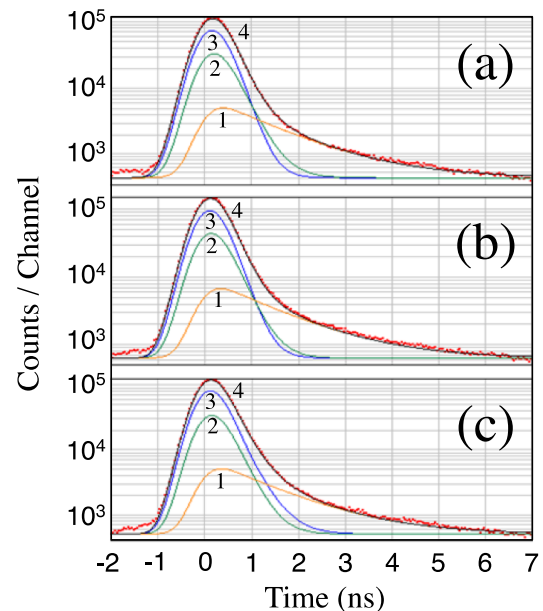


Fig. 1. Room-temperature positron lifetime spectra for single crystalline silicon (a) nonirradiated, (b) exposed to the γ -ray field of ⁶⁰Co, and (c) irradiated with thermal neutrons. See the text for each of the components 1 - 3.

Table 1. Lifetimes (ps) of positrons annihilated in the Si wafers. See the text and Fig. 1 for the alphabetic symbols (a)-(c).

Subcomponents in Si	(a)	(b)	(c)
Bulk	209 (1)	213 (1)	209 (1)
Defect	—	—	332 (2)

REFERENCE:

[1] J. Kansy, Nucl. Instr. Meth. Phys. Res. A **374** (1996) 235 - 244.

Y. Kobayashi, S. Kitao, M. Kurokuzu¹, M. Saito¹, Y. Negishi², T. Tsukuda³, N. Kojima⁴ and M. Seto

Research Reactor Institute, Kyoto University

¹Graduate School of Science, Kyoto University

²Department of Applied Chemistry, Tokyo University of Science

³Department of Chemistry, The University of Tokyo

⁴Graduate School of Arts and Sciences, The University of Tokyo

INTRODUCTION:

Metallic nanoparticles are interesting in their peculiar properties. We performed a ¹⁹⁷Au Mössbauer study to elucidate the structure and the electronic state of Au nanoparticles. In this study, we found that the Mössbauer absorption of nanoparticles is very small. The fraction of the Mössbauer absorption is proportional to the product of the absorber's thickness and the recoilless fraction. The recoilless fraction is the probability of the Mössbauer absorption, which depends on the bond strength of the Mössbauer atoms. Thus, we closely measured the Mössbauer absorption ratio of nanoparticles to elucidate the atomic bond of Au nanoparticles.

EXPERIMENTAL PROCEDURE:

Nanoparticles Au₂₅(SG)₁₈ (SG: glutathione) were prepared by reduction of Au ions and refined by electrophoreses [1]. Glutathione works as a surfactant to avoid the fusion of nanoparticles. For ¹⁹⁷Au Mössbauer measurements, the γ -ray source was ¹⁹⁷Pt in Pt foil, which was prepared by the ¹⁹⁶Pt(n, γ)¹⁹⁷Pt reaction using KUR. The spectroscopy measurements were performed at 13 K. In the spectra, zero-velocity positions were defined as the peak position for pure Au.

RESULTS AND DISCUSSION:

Fig. 1 (a) shows the ¹⁹⁷Au Mössbauer spectrum for the Au₂₅(SG)₁₈ nanoparticles. The spectrum is composed of 3 subspectra. Subspectrum 1 that shows a large quadruple splitting is due to the Au atoms making chains with the S atoms of glutathione on the surface of the nanoparticle. Subspectrum 3 shows no quadruple splitting, thus this subspectrum comes from the Au atoms that are in the core of the particle. Subspectrum 2, which is due to the Au atoms covering the core, shows a rather small quadruple splitting. The area ratio among these components is consistent with the structure of the nanoparticle [2, 3].

For the recoilless fraction determination, we measured the Mössbauer spectrum for the nanoparticles placed on Au foil, and obtained the absorption area ratio between the nanoparticles sample and the pure Au foil by fitting the spectrum. Fig. 1 (b) shows the ¹⁹⁷Au Mössbauer spectrum of the Au nanoparticles placed on a 2.5 μ m thickness Au foil. The amount of Au in the nanoparticle sample was 46 mg, and this sample was filled in a 7 mm

diameter sample case. Thus, the Au nanoparticle sample is equivalent to a 62 μ m thickness Au foil. The ratio of Au thickness between the nanoparticle sample and the Au foil is 25:1. In the observed spectrum, the absorption area for the pure Au is 31%, so the ratio of the absorption area is 2.2:1. This result means the recoilless fraction of the nanoparticles is very small, which is only 9% for the pure Au metal. The small recoilless fraction implies that the Au atomic bonds are weak or the nanoparticles move easily in the sample. To elucidate the reason for this small absorption, we are planning to measure the absorption ratio for different size nanoparticle, and compare it to the present result.

CONCLUSION:

The ¹⁹⁷Au Mössbauer spectra for Au₂₅(SG)₁₈ nanoparticles consist mainly of three components, and the area ratio of the three components shows a good agreement with a structural model. The recoilless fraction of the Au₂₅(SG)₁₈ nanoparticles is only 9% for pure Au metal.

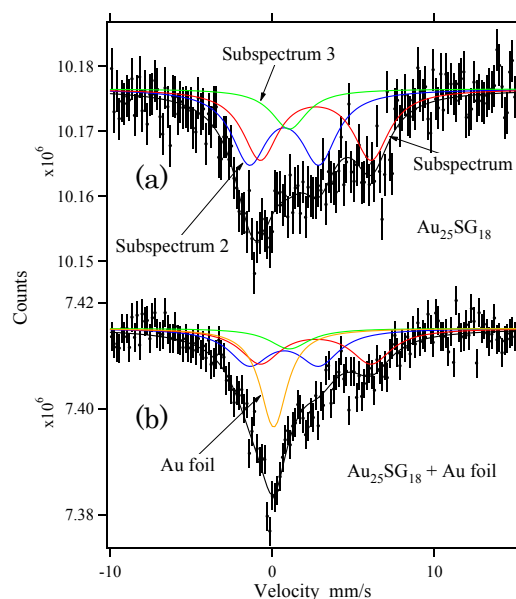


Fig. 1. ¹⁹⁷Au Mössbauer spectra for (a) Au₂₅(SG)₁₈ nanoparticles and (b) Au₂₅(SG)₁₈ nanoparticles placed on a 2.5 μ m thickness Au foil.

REFERENCES:

- [1] Y. Negishi, K. Nobusada, T. Tsukuda, J. Am. Chem. Soc. **127** (2005) 5261.
- [2] K. Ikeda, Y. Kobayashi, Y. Negishi, M. Seto, T. Iwasa, K. Nobusada, T. Tsukuda, N. Kojima, J. Am. Chem. Soc. **129** (2007) 7230.
- [3] T. Tsukuda, Y. Negishi, Y. Kobayashi, N. Kojima, Chem. Lett. **40** (2011) 1292-1293.

PR10-7 Elucidation of a Correlation between Magnetic Properties and Guest Inclusion in Magnetically Bistable Porous Coordination Polymers

M. Ohba, R. Ohtani¹, M. Arai¹, S. Kitao² and M. Seto²

Department of Chemistry, Faculty of Science, Kyushu University

¹Graduate School of Engineering, Kyoto University

²Research Reactor Institute, Kyoto University

INTRODUCTION: Porous coordination polymers (PCPs) are a new type of guest adsorbent material consisting of flexible coordination bonds to provide permanent and designable regular porous structures [1]. Such PCPs are expected to be multifunctional platforms combining porous properties with specific chemical and physical properties. To couple the magnetic properties and the porous properties we have researched PCPs exhibiting spin transition (ST). $\{\text{Fe}^{\text{II}}(\text{pz})[\text{Pd}^{\text{II}}(\text{CN})_4]\}$ (**1**; pz = pyrazine) shows ST near room temperature with a hysteresis width of 20 K ($T_c^\uparrow = 304$ K and $T_c^\downarrow = 284$ K). The ST behavior of **1** could be controlled through guest inclusion [2]. An iodine clathrate **1**⊃**I** was obtained by exposing the guest-free compound **1** to iodine vapor. **1**⊃**I** exhibited ST with a hysteresis width of 117 K ($T_c^\uparrow = 320$ K and $T_c^\downarrow = 203$ K), which means drastic enhancement of cooperativity by the iodine inclusion. To elucidate the mechanism of the enhancement cooperativity, we investigated the chemical state and distribution of iodine molecules in the pores by ¹²⁹I-Mössbauer spectroscopy. Because ¹²⁹I-Mössbauer spectroscopy is available below 80 K due to effect of large lattice vibration, the spectrum of **1**⊃**I** in the high spin state cannot be obtained. For deeper discussions, a nickel analog $\{\text{Ni}^{\text{II}}(\text{pz})[\text{Pd}^{\text{II}}(\text{CN})_4]\}$ (**2**) and its iodine clathrate (**2**⊃**I**) having corresponding frameworks to **1** and **1**⊃**I** in the high spin state were prepared as alternate samples.

EXPERIMENTS: **1**⊃**I** and **2**⊃**I** included ¹²⁹I were prepared by using ¹²⁹I₂ produced by heating to Pd¹²⁹I₂. ¹²⁹I-Mössbauer spectroscopy was measured to use Zn¹²⁹Te as radiation source at around 15 K under He atmosphere.

RESULTS: As shown in Fig. 1, **2**⊃**I** showed broader peaks in comparison with the spectrum of **1**⊃**I**, indicating that the iodine existed at many sites with wide distribution in the pores incommensurately. In the high spin state, each iodine molecule was affected by the different environments of the pore surface and gave the broad spectrum with diverse values of isomer shift (IS) and quadrupole coupling constant (QCC). On the other hand, **1**⊃**I** in the low spin state gave a narrow spectrum because these iodine molecules were fixed in the pores commensurately. The different arrangement of iodine between **1**⊃**I** and **2**⊃**I** was confirmed by X-ray powder

diffraction patterns. The spectrum of **1**⊃**I** was simulated with three kinds of octuplets, indicating that three chemically independent iodine sites existed in the pores. Site 1 had slight positive charge (IS = 0.95 mm s⁻¹, QCC = -2540 MHz) with occupancy of 14.5 %. Site 2 was a main component with neutral charge (IS = 1.00 mm s⁻¹, QCC = -2290 MHz) and occupancy of 76.3 %. Site 3 was a minor component having slight negative charge (IS = 0.68 mm s⁻¹, QCC = -1660 MHz) and occupancy of 9.2 %. Total charge of iodine was zero. Most of the iodine existed as I₂ and a part of the iodine showed charge separation in the pores of **1**⊃**I**.

These results suggested that the iodine molecules interacted with various sites in the pore and showed a charge fluctuation originated from different host-guest interactions. The enhancement of cooperativity in **1**⊃**I** could be explained by the change of interactions between iodine and framework associated with the ST.

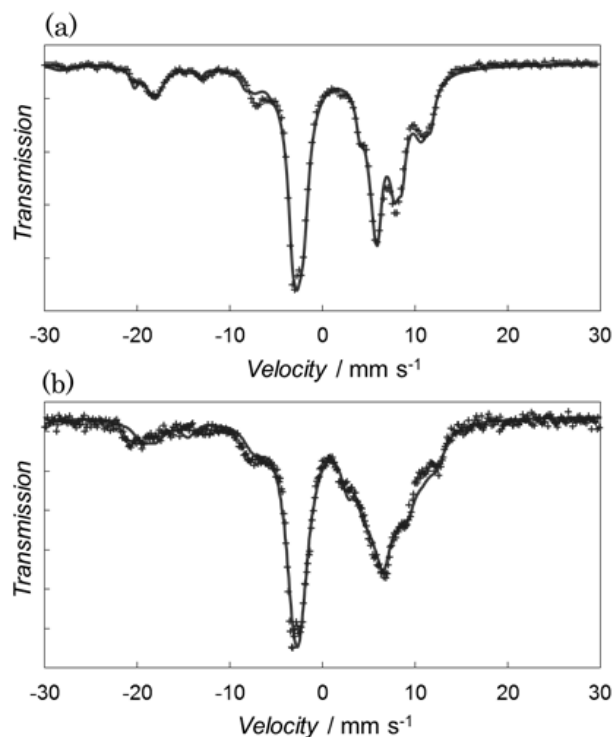


Fig. 1. ¹²⁹I-Mössbauer spectra of (a) **1**⊃**I** in the low spin state and (b) **2**⊃**I** corresponding to the framework in the high spin state at 15 K; observed (dots) and simulation (line).

REFERENCES:

- [1] S. Kitagawa *et al.*, *Angew. Chem. Int. Ed.* **43** (2004) 2334-2375.
- [2] M. Ohba *et al.*, *Angew. Chem. Int. Ed.* **48** (2009) 4767-4771.

T. Yokoyama, Y. Okaue, D. Kawamoto, H. Ohashi¹ and Y. Kobayashi²

Faculty of Sciences, Kyushu University

¹Center for Research and Advancement in Higher Education, Kyushu University

²Research Reactor Institute, Kyoto University

INTRODUCTION: Gold nanoparticles supported on nickel oxide have been used as various oxidation-reduction catalysts [1]. It is essential to characterize the catalysts for understanding their advantages and establishing guidelines for syntheses of catalysts with high activity. For the characterization of supported gold catalysts, the oxidation states of the supported gold nanoparticles have been determined by X-ray absorption spectroscopy (XAS) and their crystal phases have been detected by powder X-ray diffraction (XRD). However, supported gold catalysts have rarely been characterized by ^{197}Au Mössbauer spectroscopy.

In this study, the detailed chemical state of a supported gold catalyst was found using ^{197}Au Mössbauer spectroscopy, in addition to the oxidation states and structures of various metals having been obtained by XAFS.

EXPERIMENTS: Supported gold catalysts (Au/NiO_x) were prepared by the coprecipitation method. An aqueous mixed solution of HAuCl_4 and $\text{Ni}(\text{NO}_3)_2$ was poured into an NaOH solution under stirring. The precipitates were filtered, washed and freeze dried. The obtained materials were calcined in air (Au/NiO_x (air)) or were reduced in a flow of H_2 gas (Au/NiO_x (H_2)) at 573 K for 4 h.

The chemical state of gold in the solid samples obtained was determined by ^{197}Au Mössbauer spectroscopy (home-made equipment). The ^{197}Pt isotope ($T_{1/2} = 18.3$ h), a γ -ray source feeding the 77.3-keV Mössbauer transition of ^{197}Au , was prepared by neutron irradiation of isotopically enriched ^{196}Pt metal at the Kyoto University Reactor. The absorbers were particle specimens. The source and specimens were cooled with a helium refrigerator. The temperature of the specimens was in the range 8 – 15 K. The zero velocity point of the spectra was the peak point of pure bulk gold. The spectra for all the solid samples were fitted with a single Lorentzian function.

Furthermore, for these catalysts, Ni-K edge and Au-L₃ edge XAFS were measured at BL14B2 of SPring-8 (Hyogo, Japan).

RESULTS: The Ni-K XANES spectra for the Au/NiO_x (H_2) catalyst revealed that most of the nickel oxide was

reduced to nickel metal. The Au-L₃ XANES spectra for the Au/NiO_x (H_2) catalyst confirmed the presence of Au(0). However, the Au(0) was different from bulk Au, suggesting the formation of new phases. Fig. 1 shows the ^{197}Au Mössbauer spectra for the Au/NiO_x catalysts. From the ^{197}Au Mössbauer spectrum for Au/NiO_x (H_2), it can be reasonably expected that AuNi_x alloy phases were formed by hydrogen reduction [2]. The combination of XAS and ^{197}Au Mössbauer spectroscopy is quite useful to characterize supported gold catalysts.

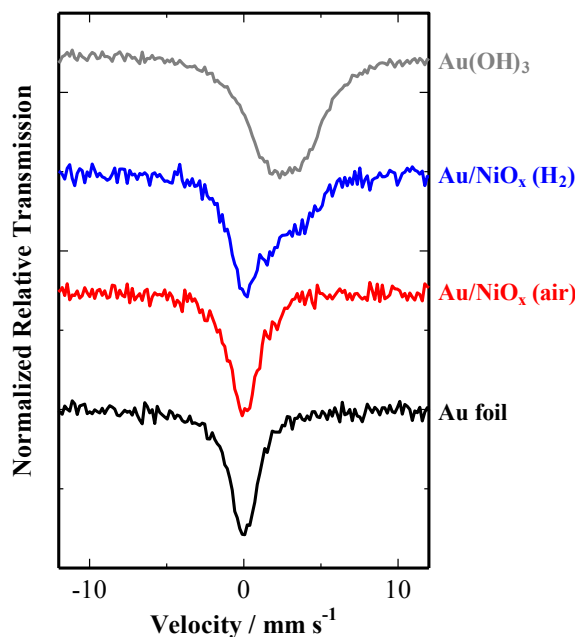


Fig. 1. ^{197}Au Mössbauer spectra for the Au/NiO_x catalysts.

REFERENCES:

- [1] H. Nishikawa et al., *Adv. X-Ray. Chem. Anal. Jpn.* **43** (2012) 285-292.
- [2] D. Kawamoto et al., *Adv. X-Ray. Chem. Anal. Jpn.* **43** (2012) 293-302.